

Synthesis and characterisation of liposomal doxorubicin with loaded gold nanoparticles

ISSN 1751-8741
 Received on 18th December 2017
 Revised 11th March 2018
 Accepted on 31st March 2018
 E-First on 22nd May 2018
 doi: 10.1049/iet-nbt.2017.0321
 www.ietdl.org

Ali Akbar Karimi Zarchi¹, Seyed Mohamad Amini^{2,3} ✉, Ali Salimi¹, Sharmin Kharazi⁴

¹Nanobiotechnology Research Center, Baqiyatallah University of Medical Sciences, Tehran, Iran

²Radiation Biology Research Center, Iran University of Medical Sciences (IUMS), Tehran, Iran

³Department of Medical Nanotechnology, School of Advanced Technologies in Medicine, Iran University of Medical Sciences (IUMS), Tehran, Iran

⁴Department of Medical Nanotechnology, School of Advanced Technologies in Medicine (SATIM), Tehran University of Medical Sciences (TUMS), Tehran, Iran

✉ E-mail: m_aminirazi@razi.tums.ac.ir

Abstract: Developing nanostructures for cancer treatment is growing significantly. Liposomal doxorubicin is a drug that is used in the clinic and represents a lot of benefits over doxorubicin. The development of multifunctional liposomes with different cancer treatment capability enables broader applications of doxorubicin chemotherapy. Many efforts were carried to prepare more effective liposomal formulation through loading gold nanoparticles (GNPs) in the formulation. Here, GNPs with an average size of 6 nm were loaded in liposomal formulation alongside doxorubicin. The hydrodynamic diameter of final formulation was 177.3 ± 33.9 nm that in comparison with liposomes without GNPs (112.5 ± 10.3 nm), GNPs-loaded liposomes showed the bigger hydrodynamic diameter. GNPs-loaded liposomes are slightly positively charged (4.4 ± 1.1 mV), while liposomes without loading the GNPs were negatively charged (-18.5 ± 1.6 mV). Doxorubicin was loaded in this formulation through active loading technique. Doxorubicin loading efficiency in gold-loaded liposomes is slightly lesser than liposomes without GNPs, but still considerably high in comparison to passive loading techniques.

1 Introduction

Cancer is one of the major cause of death worldwide. Many of researchers and physicians around the world are working continuously in the field of cancer prevention, detection, diagnosis, imaging, and therapy. Cancer nanotechnology has the potential to bring new approaches in different cancer diagnostic and treatment. Advancement in nanomaterial science provides radio sensitizers [1] and nanocarriers [2] which led to better chemotherapy and radiotherapy treatment. Gold nanoparticles (GNPs) with unique properties such as biocompatibility, antioxidant activity, surface plasmons resonance (SPR), and surface-enhanced Raman scattering and X-ray opacity (as a result of high Z) have been introduced as a useful nano platform for different diagnostics [3, 4] and therapeutics applications [5, 6]. Cancer hyperthermia [7], photodynamic therapy [8], and immunotherapy [9] have been revolutionised by newly introduced nanomaterial.

Liposome is one of the main nanocarriers that have been approved for clinical cancer chemotherapy [10]. Pegylated nanoliposomes are representing many qualities for cancer drug delivery. These nanostructures are stable enough to prevent drug leakage while in circulation. Pegylated nanoliposomes could avoid reticuloendothelial system and reach the tumour area based on enhanced permeability and retention effect [11]. Currently, liposomal doxorubicin is in market under trade name of Doxil[®], Caelyx[®], and Myocet[®]. This drug was used for AIDS-related Kaposi's sarcoma, breast cancer, ovarian cancer, and other solid tumours [12]. However, the lack of control over drug release form it [13], and induce multi-drug resistances in some cases of cancers as a result of slow doxorubicin release, make the conventional liposomal doxorubicin impotent [14].

Feasibility of bonding metal and organic [15], or inorganic nanostructures [16] was investigated for different biomedical application. Preparation of liposomal doxorubicin with bonded or encapsulated GNPs is very interesting. Apart from overcoming the problem of drug release from the pegylated liposome through light exposure and trigger release strategy [17], such a formulation could

be applicable for combination of photo thermal and radiation therapy with chemotherapy.

Based on our knowledges, all the liposomal formulation that incorporated with GNPs used passive doxorubicin loading techniques. Herein, we introduce new liposome–GNPs complex. Our report contains investigation of the pegylated liposomes–gold complex and doxorubicin encapsulation efficiency. Lipid composition was similar to commercially available Doxil[®] formulation to prepare stable liposome formulation of doxorubicin that has minimum unwanted leakage of drug that may cause the systemic side effect. As a result of GNPs presence, this formulation could be a great X-ray contrast agent for computed tomography and radiosensitisation agent for combination radiotherapy and chemotherapy treatment of cancer. Also, hyperthermia and stimulus release of doxorubicin could be achieved by laser irradiation of GNPs.

2 Material and methods

2.1 Materials

Methoxypolyethylene glycol (MW 2000)-distearoylphosphatidylcholine (mPEG2000-DSPE), hydrogenated soy phosphatidylcholine (HSPC), and cholesterol (Chol) were obtained from Avanti Polar Lipids (Alabaster, AL, USA). Gold (III) chloride trihydrate ($\text{HAuCl}_4 \cdot 3\text{H}_2\text{O}$, 99.9%), cetyltrimethylammonium bromide (CTAB, 97%), hydrochloric acid (HCl, ACS reagent, 37%) and nitric acid (HNO_3 , ACS reagent, 65%), ethanol, methanol, and chloroform were purchased from Merck (Darmstadt, Germany). By adding 7.5 ml HCl 1 M and 2.5 ml water to 90 ml isopropanol (Merck, Darmstadt, Germany), acidified isopropyl alcohol (90% isopropanol/0.075 M HCl) was prepared. All solutions were prepared with DI water (Barnsted E-PureTM 18.3 M Ω). Glasswares were cleaned with aqua regia and rinsed thoroughly with DI water.

2.2 Synthesis of GNPs

CTAB-capped GNPs were synthesised by using the chemical method based on our previous reports [18]. Briefly, 0.5 ml solution of CTAB (0.1 M) was mixed with 12 ml solution of $\text{HAuCl}_4 \cdot 3\text{H}_2\text{O}$ (0.001 M). Then, 0.5 ml solution of fresh ice-cold sodium borohydride (0.1 M) was injected into the prepared solution and stirred vigorously for 15 min. The final CTAB concentration in GNPs solution is 3.8 mM. CTAB-capped GNPs have been concentrated through sequences of centrifugation with 50 kDa centrifugation filter tube at 3000 rpm for 4 min.

2.3 Preparation of GNPs encapsulated liposome

From stock solutions, HSPC, cholesterol, and mPEG2000-DSPE have been poured into a glass tube in molar ratios of 55:40:5. Chloroform was evaporated with a rotary evaporator and subsequently with 2 h connection to freeze-dryer lipids were dried completely. Liposomes without GNPs were prepared based on thin films hydration method and downsized by sonication and extrusion as it has been reported [19].

However, for the preparation of GNP-bonded liposomes, under an argon atmosphere at 65°C, 10 mg/ml lipid film was hydrated in a solution of GNPs (1500 µg/ml) and ammonium sulphate (250 mM). For the preparation of this hydration solution, proper weight of ammonium sulphate salt was dissolved in aqueous solution of GNPs (1500 µg/ml), in a manner that final mixture contains 250 mM ammonium sulphate and 1500 µg/ml gold ion. After 15 min of sonication, series of extrusion through polycarbonate membranes of 400, 200, and 100 nm, in a sequence, was performed.

2.4 Characterisation of liposomes GNPs and of GNPs-loaded liposomes

According to separate free ammonium sulphate ions, liposomes were dialysed against 5% w/v dextrose solution. Based on Bartlett phospholipid assay, the mass of total lipid concentration was determined [20]. With remote loading method, doxorubicin was encapsulated in liposomes using ammonium sulphate concentration gradient, based on previous report [21]. Briefly, ammonium sulphate encapsulated liposomes were incubated with doxorubicin solution (2 mg doxorubicin per 10 µmol of total lipid) for 1 h at 65°C, then cooled to room temperature, in order to remove free doxorubicin molecules, the solution was mixed with Dowex[®] resin and rotated for 1 h. Concentration of doxorubicin was calculated by fluorimetry as was reported by Amselem *et al.* [22].

Transmission electron microscopy (TEM) micrographs of nanostructures were recorded by Zeiss EM 900 microscope operated at 80 kV without any staining. Liposomes formulation has been stained with 2% uranyl acetate solution. An excess of staining solution was removed with filter paper in 1 min. Zeta potential, average hydrodynamic diameter, and polydispersity index (PDI) were investigated by Malvern Nanosizer dynamic light scattering (DLS) (Malvern Instrument, UK) in natural pHs. UV-Visible absorption spectroscopy has performed with 1 cm of optical path length quartz cuvette [SPEKOL 2000 double beam UV-Visible spectrophotometer (Analytik Jena, UK)]. Inductively coupled plasma atomic emission spectroscopy (VISTA-PRO, Varian, Australia) has been used for gold ion concentration measurements. Doxorubicin concentration measurements were carried out by spectrofluorimeter (Jasco FP-6200, USA).

2.5 Encapsulation efficiency analysis

The efficiency of doxorubicin encapsulation in prepared liposome was studied after removing unloaded doxorubicin with Dowex[®] resin based on Amselem *et al.* [22]. A liposomal formulation containing doxorubicin was lysed with acidified isopropyl alcohol then doxorubicin concentration was extrapolated according to a standard curve. A standard curve of doxorubicin solution has been obtained by fluorimetry (λ_{Ex} : 470 nm, λ_{Em} : 550 nm). The followed formula was used for encapsulation efficiency calculations (three repetitions have been performed for every experiment)

Encapsulation efficiency

$$= \frac{\text{Dox conc} \cdot \text{before Dowex}}{\text{Dox conc} \cdot \text{after Dowex purification}} \times 100$$

2.6 Statistical analysis

Data were analysed and depicted with GraphPad Prism 6 (GraphPad Software, San Diego, CA, USA), and Origin 2015 (OriginLab Co., USA) software. The mean ± standard deviation was represented in diagrams. Groups were compared with Student's *t*-test. Differences are considered significant statistically when probability $P < 0.05$.

3 Results and discussion

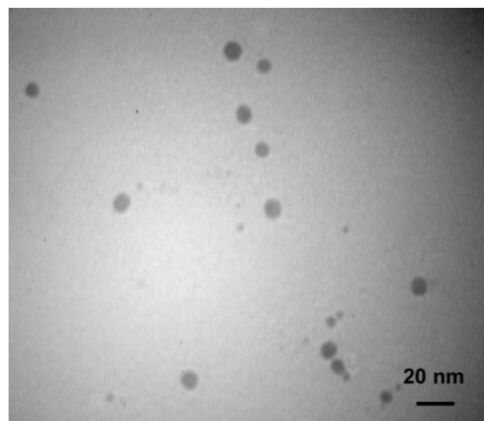
Based on Mandal *et al.*'s report for preparation of metal oxide nanoparticles, the concentration of surfactant must be chosen with regard to critical micelle concentration [23]. So, 0.1 M of CTAB concentration was used and synthesis of positively charged GNPs has been performed. According to the method introduced by Haiss that apply UV-Vis spectrum for determination of GNPs size [24], the average size of nanoparticles is 6 nm [(Fig. 1d) (λ_{SPR} : 513 nm, $A_{\text{SPR}}/A_{450\text{nm}} \sim 1.31$)] which is in good agreement with TEM micrograph of CTAB GNPs (Fig. 1a). Based on our previous study, the diameter of GNPs was 7.3 ± 7.1 nm [18].

As a result of CTAB presence at the surface of GNPs, they are positively charged [25] and they could interact with negatively charged liposomes with electrostatic interaction. In TEM micrographs, GNPs were observed in boundary surface within the liposomal membrane which indicates the electrostatic interaction between GNPs and liposomal membrane (Fig. 1c).

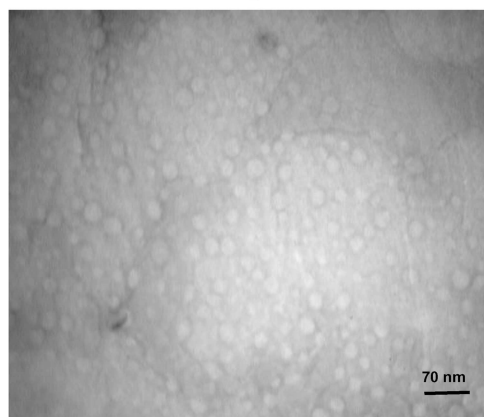
The increase in size and hydrodynamic diameter of liposomes was observed in TEM micrographs and DLS results after GNPs electrostatic bond to the liposomal membrane (Fig. 2). Two peaks were observed in most of hydrodynamic diameter distribution diagram. The main peak (209.3 ± 79.1 nm) represents the liposomal formulation but smaller peak (29.9 ± 20.2 nm) could represent the GNPs or smaller liposomes. Similar DLS results for gold nanorods bonded liposomes were reported by Lozano *et al.* [26]. The hydrodynamic diameter of prepared liposome without GNPs was 112.5 ± 10.3 nm which is smaller than GNPs bonded liposomes. This difference in size between two formulations is a direct result of differences in extrusion process because of high viscosity and possible aggregation of GNPs inside the pores polycarbonate membranes. Free liposomes were extruded easily even with 50 nm polycarbonate membranes but GNPs-loaded liposomes extrusion process was hardly done with 100 nm membranes. The increase in hydrodynamic sizes of GNP-loaded liposomes in comparison of liposomes without GNPs was reported by others [27–29].

Fig. 1d shows the UV-Vis spectra of GNPs and GNPs-loaded liposomes. UV-Vis spectra of liposomal formulation represent the SPR peak clearly, which indicated that GNPs were not aggregated in the formulation. The small red shift of SPR peak of GNPs was observed that could be as a result of lipid interaction. The increase in absorption value for GNPs in liposomes complex is a result of hydrophobic (lipid bilayer) environment around GNPs which has been reported by Lozano *et al.* for the complex of liposomes and gold nanorods [26].

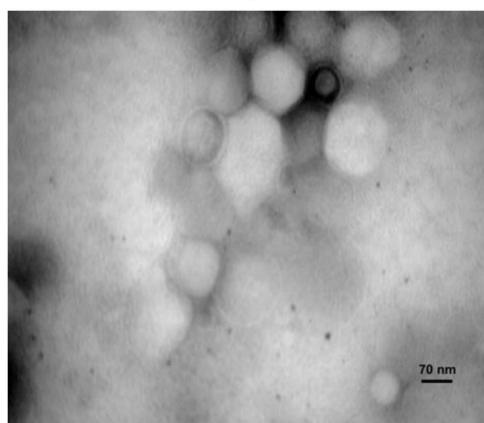
CTAB covered GNPs are positively charged and could easily interact with the negatively charged membrane of liposomes. Liposomes zeta potential is -18.5 ± 1.6 mV but after attaching GNPs to liposomes, zeta potential was increased up to $+4.4 \pm 1.1$ mV. This is clearly represented by the electrostatic bond between the positively charged GNP and negatively charged liposomes. Mady *et al.* [30] investigate the zeta potential of loaded GNPs with liposomes. They use negatively charged nanoparticles for loading and report negative zeta potential of liposomes is increased because of surface bonded negatively charged GNPs. In another report by Pornpattananangkul *et al.* [31], cationic liposomes were binded by negatively charged GNPs (4 nm) then surface charge converted to negative values.



a



b



c

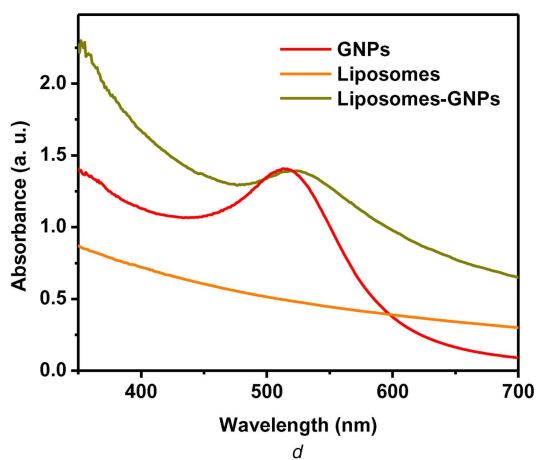


Fig. 1 TEM micrographs of (a) GNPs, (b) Liposomes, (c) GNPs-liposomes complexes, (d) UV-VIS spectra of synthesised GNPs, liposomes, and GNPs-liposomes complexes

In comparison to passive loading technique, remote loading of doxorubicin in liposomal formulation provide much higher

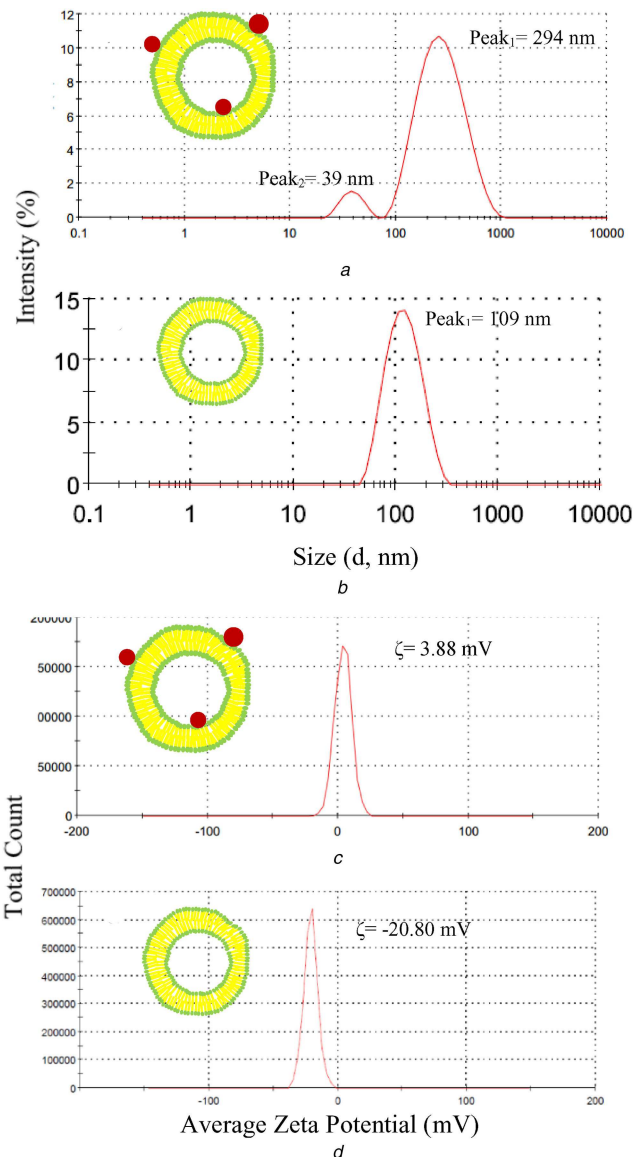


Fig. 2 Hydrodynamic diameter distribution (by intensity) of (a) Gold-loaded liposomes, (b) Liposomes, (c) Zeta potential distribution of gold-liposomes formulations, (d) Liposomes

doxorubicin encapsulation efficiency. One of the most common remote loading techniques for doxorubicin is through an ammonium sulphate gradient which has been applied for commercial Doxil[®] product [11]. Remote loading encapsulation efficiency is 98–100% in Mayer *et al.*'s report [32]. Also, used lipid composition (HSPC, cholesterol, and mPEG2000-DSPE) leads to a very stable formulation with lowest drug release based on previous release investigation [22].

Incorporation of gold nanoshells encapsulated in giant unilamellar liposomes with thermosensitive lipids was performed by Zasadzinski *et al.* [17]. Their formulation is much larger than commercial liposomal doxorubicin with encapsulated carboxyfluorescein with passive loading technique. In our samples, the average percentage of doxorubicin encapsulation is liposomal formulation is 93.71%. The average encapsulation efficiency for GNP-liposome complex is 87.44%, which is significantly lower than formulation without GNPs (Fig. 3). Mathiyazhakan *et al.* [33] report that casein passive loading efficiency was decreased as a result of GNPs presence in liposomes formulation. Based on Pradhan *et al.* [27], results remote doxorubicin loading efficiency of liposomes with loaded magnetic nanoparticles was decreased in comparison to liposomes without magnetic nanoparticles down to 85%. These reports alongside our results indicate that co-encapsulation of nanoparticles and drugs in liposomal formulation lead to lower drug encapsulation.

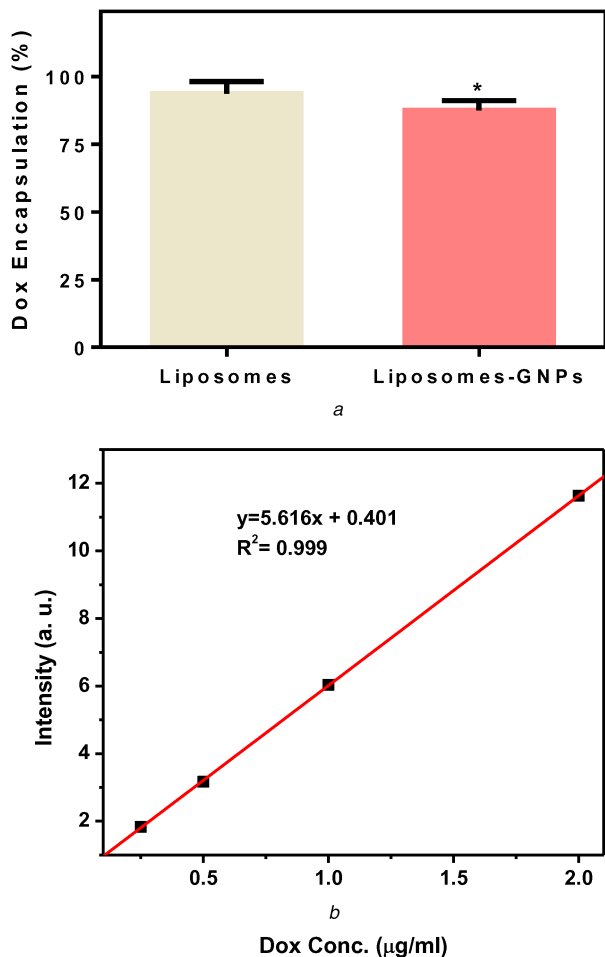


Fig. 3 Doxorubicin encapsulation efficiency in (a) Liposomal formulation, (b) The standard curve of doxorubicin. A standard curve was used to estimate the amount of doxorubicin after liposomes formulation lysis by acidified isopropyl alcohol

4 Conclusion

Positively charged GNPs (6 nm) and negatively charged liposomes were synthesised and characterised. Therefore, GNPs were loaded in conventional liposomal formulation of doxorubicin. GNPs-loaded liposomes are slightly positively charged and have higher hydrodynamic diameter, while liposomes without loading, the GNPs were negatively charged and have a smaller hydrodynamic diameter. Doxorubicin was encapsulated in liposomes with remote loading technique through using ammonium sulphate concentration gradient. Loading efficiency in gold-loaded liposomes is slightly lesser than liposomes without GNPs but still considerably high.

5 References

[1] Mesbahi, A.: 'A review on gold nanoparticles radiosensitization effect in radiation therapy of cancer', *Rep. Pract. Oncol. Radiother.*, 2010, **15**, (6), pp. 176–180

[2] Cui, W., Li, J., Decher, G.: 'Self-assembled smart nanocarriers for targeted drug delivery', *Adv. Mater.*, 2016, **28**, (6), pp. 1302–1311

[3] Emami, T., Madani, R., Golchinfar, F., *et al.*: 'Comparison of gold nanoparticle conjugated secondary antibody with non-gold secondary antibody in an ELISA kit model', *Monoclon. Antib. Immunodiagn. Immunother.*, 2015, **34**, (5), pp. 366–370

[4] Fatemi, F., Amini, S.M., Kharrazi, S., *et al.*: 'Construction of genetically engineered M13K07 helper phage for simultaneous phage display of gold binding peptide 1 and nuclear matrix protein 22 ScFv antibody', *Colloids Surf. B. Biointerfaces*, 2017, **159**, (Suppl. C), pp. 770–780

[5] Darabpour, E., Kashef, N., Amini, S.M., *et al.*: 'Fast and effective photodynamic inactivation of 4-day-old biofilm of methicillin-resistant *Staphylococcus aureus* using methylene blue-conjugated gold nanoparticles', *J. Drug Deliv. Sci. Technol.*, 2017, **37**, pp. 134–140

[6] Shaabani, E., Amini, S.M., Kharrazi, S., *et al.*: 'Curcumin coated gold nanoparticles: synthesis, characterization, cytotoxicity, antioxidant activity and its comparison with citrate coated gold nanoparticles', *Nanomedicine J.*, 2017, **4**, (2), pp. 115–125

[7] Amini, S.M., Kharrazi, S., Jaafari, M.R.: 'Radio frequency hyperthermia of cancerous cells with gold nanoclusters: an in vitro investigation', *Gold Bull.*, 2017, **50**, (1), pp. 43–50

[8] Amini, S.M., Kharrazi, S., Hadizadeh, M., *et al.*: 'Effect of gold nanoparticles on photodynamic efficiency of 5-aminolevulinic acid photosensitiser in epidermal carcinoma cell line: an in vitro study', *IET Nanobiotechnol.*, 2013, **7**, (4), pp. 151–156

[9] Almeida, J.P.M., Figueroa, E.R., Drezek, R.A.: 'Gold nanoparticle mediated cancer immunotherapy', *Nanomed. Nanotechnol. Biol. Med.*, 2014, **10**, (3), pp. 503–514

[10] Kim, J.-S.: 'Liposomal drug delivery system', *J. Pharm. Invest.*, 2016, **46**, (4), pp. 387–392

[11] Allen, T.M., Cullis, P.R.: 'Liposomal drug delivery systems: from concept to clinical applications', *Adv. Drug Deliv. Rev.*, 2013, **65**, (1), pp. 36–48

[12] Wibroe, P.P., Ahmadvand, D., Oghabian, M.A., *et al.*: 'An integrated assessment of morphology, size, and complement activation of the PEGylated liposomal doxorubicin products Doxil®, Caelyx®, DOXOrubicin, and SinaDoxosome', *J. Controlled Rel.*, 2016, **221**, pp. 1–8

[13] Barenholz, Y.: 'Liposome application: problems and prospects', *Curr. Opin. Colloid Interface Sci.*, 2001, **6**, (1), pp. 66–77

[14] Szakács, G., Paterson, J.K., Ludwig, J.A., *et al.*: 'Targeting multidrug resistance in cancer', *Nat. Rev. Drug Discov.*, 2006, **5**, p. 219

[15] Mandal, A., Sekar, S., Seeni Meera, K.M., *et al.*: 'Fabrication of collagen scaffolds impregnated with sago starch capped silver nanoparticles suitable for biomedical applications and their physicochemical studies', *Phys. Chem. Chem. Phys.*, 2014, **16**, (37), pp. 20175–20183

[16] Das, S.K., Khan, M.M., Parandhaman, T., *et al.*: 'Nano-silica fabricated with silver nanoparticles: antifouling adsorbent for efficient dye removal, effective water disinfection and biofouling control', *Nanoscale*, 2013, **5**, (12), pp. 5549–5560

[17] Wu, G., Mikhailovsky, A., Khant, H.A., *et al.*: 'Remotely triggered liposome release by near-infrared light absorption via hollow gold nanoshells', *J. Am. Chem. Soc.*, 2008, **130**, (26), pp. 8175–8177

[18] Amini, S.M., Kharrazi, S., Rezayat, S.M., *et al.*: 'Radiofrequency electric field hyperthermia with gold nanostructures: role of particle shape and surface chemistry', *Artif. Cells, Nanomed., Biotechnol.*, 2017, pp. 1–11, DOI: <https://doi.org/10.1080/21691401.2017.1373656>

[19] de Menezes, D.E.L., Pilarski, L.M., Allen, T.M.: 'In vitro and in vivo targeting of immunoliposomal doxorubicin to human B-cell lymphoma', *Cancer Res.*, 1998, **58**, (15), pp. 3320–3330

[20] Bartlett, G.R.: 'Phosphorus assay in column chromatography', *J. Biol. Chem.*, 1959, **234**, pp. 466–468

[21] Bolotin, E.M., Cohen, R., Bar, L.K., *et al.*: 'Ammonium sulfate gradients for efficient and stable remote loading of amphiphatic weak bases into liposomes and ligandoliposomes', *J. Liposome Res.*, 1994, **4**, (1), pp. 455–479

[22] Amselem, S., Gabizon, A., Barenholz, Y.: 'Optimization and upscaling of doxorubicin-containing liposomes for clinical use', *J. Pharm. Sci.*, 1990, **79**, (12), pp. 1045–1052

[23] Fathima, N.N., Rajaram, A., Sreedhar, B., *et al.*: 'The formation of copper oxide nanorods in the presence of various surfactant micelles', *Indian J. Sci. Technol.*, 2008, **1**, (7), pp. 1–6

[24] Haiss, W., Thanh, N.T.K., Aveyard, J., *et al.*: 'Determination of size and concentration of gold nanoparticles from UV–Vis spectra', *Anal. Chem.*, 2007, **79**, (11), pp. 4215–4221

[25] Lin, J., Zhou, W., O'Connor, C.J.: 'Formation of ordered arrays of gold nanoparticles from CTAB reverse micelles', *Mater. Lett.*, 2001, **49**, (5), pp. 282–286

[26] Lozano, N., Al-Jamal, W., Taruttis, A., *et al.*: 'Liposome-gold nanorod hybrids for high-resolution visualization deep in tissues', *J. Am. Chem. Soc.*, 2012, **134**, (32), pp. 13256–13258

[27] Pradhan, P., Giri, J., Rieken, F., *et al.*: 'Targeted temperature sensitive magnetic liposomes for thermo-chemotherapy', *J. Controlled Rel.*, 2010, **142**, (1), pp. 108–121

[28] Xia, Y., Qi, S., Zhang, X., *et al.*: 'Construction of thermal-and light-responsive liposomes noncovalently decorated with gold nanoparticles', *RSC Adv.*, 2014, **4**, (84), pp. 44568–44574

[29] Demir, B., Barlas, F.B., Guler, E., *et al.*: 'Gold nanoparticle loaded phytosomal systems: synthesis, characterization and in vitro investigations', *RSC Adv.*, 2014, **4**, (65), pp. 34687–34695

[30] Mady, M.M., Fathy, M.M., Youssef, T., *et al.*: 'Biophysical characterization of gold nanoparticles-loaded liposomes', *Physica Medica*, 2012, **28**, (4), pp. 288–295

[31] Pornpattananangkul, D., Olson, S., Aryal, S., *et al.*: 'Stimuli-responsive liposome fusion mediated by gold nanoparticles', *ACS Nano*, 2010, **4**, (4), pp. 1935–1942

[32] Mayer, L., Bally, M., Cullis, P.: 'Uptake of Adriamycin into large unilamellar vesicles in response to a pH gradient', *Biochim. Biophys. Acta (BBA)-Biomembranes*, 1986, **857**, (1), pp. 123–126

[33] Mathiyazhakan, M., Yang, Y., Liu, Y., *et al.*: 'Non-invasive controlled release from gold nanoparticle integrated photo-responsive liposomes through pulse laser induced microbubble cavitation', *Colloids Surf. B. Biointerfaces*, 2015, **126**, (Suppl. C), pp. 569–574